ELSEVIER

Journal of Nuclear Materials 306 (2002) 173–179

journal of nuclear materials

www.elsevier.com/locate/jnucmat

Radiogenic silicon precipitates in neutron irradiated aluminum

E. Brosh, A. Kiv *

Department of Materials Engineering, Ben-Gurion University of the Negev, P.O. Box 653, Beer Sheva 84104, Israel

Received 28 May 2002; accepted 16 September 2002

Abstract

A theory of precipitation of radiogenic Si in Al is developed. The aim of this study is to predict quantitatively the variation of microstructural parameters such as precipitates number and sizes dependently on irradiation parameters. Analogy with deposition of thin films and formation of silver halides is discussed. A model for the precipitation of radiogenic Si in Al is developed on the basis of the theory of Ostwald-ripening in precipitation processes with constant rate addition of monomers. The model predicts that after the precipitation process enters the 'late' stage, the number of precipitates depends only on the ratio between the thermal and fast neutron fluxes but not on the absolute values of flux and fluence. A quantitative interpretation of the *spectral effect*, suggested by Farrell [Mater. Res. Soc. Symp. Proc. 373 (1995) 165] is given. The predictions of the model are compared with experimental results.

1. Introduction

In neutron-irradiated aluminum Si is produced by (n,γ) transmutation reaction, initiated by thermal neutrons. The solubility of Si in Al at the irradiation temperatures is negligible and therefore the radiogenic Si segregates into precipitates, in particular with diamond structure [1,2]. Along with void-formation, caused by fast-neutrons, Si precipitates increase the material's strength and decrease its ductility [3]. The mechanical properties may depend not only on the whole amount of produced Si but also on the precipitate size and number. Thus it is important to know the dependence of Si precipitates size and number on irradiation conditions.

Recently, Farrell [4] analyzed experimental results obtained at two reactors and suggested the existence of a 'spectral effect', which is revealed in the dependence of the number and sizes of precipitates on the spectrum of reactor neutrons. Farrell argued that vacancies formed by fast neutrons increase the diffusion coefficient, therefore, the precipitates size and number depend not only on the thermal neutron fluence, but also on the fast neutron fluence. In the present paper we consider the late stage of precipitate growth with the constant addition of Si atoms due to transmutation and evaluate the spectral effect.

2. Nucleation and growth with constant addition of monomers

2.1. Constant-composition and changing-composition systems

A precipitation process may be initiated by changing external conditions, such as quenching a solution from high temperature to a lower temperature at which the solution is metastable. In these systems the system composition does not change during the precipitation. In [5] such systems are called 'conservative systems'. These processes are described by the theories of nucleation and growth, for example, the comprehensive theory recently developed by Slezov and Schmelzer [6].

In contrast, the precipitation of radiogenic Si in Al is an example for a changing-composition system because the segregating monomers (Si atoms) are gradually produced, so that the atomic fractions of Al and Si in

---

* Corresponding author. Tel./fax: +972-8 6461460.
E-mail address: kiv@bgumail.bgu.ac.il (A. Kiv).

0022-3115/02/$ - see front matter © 2002 Elsevier Science B.V. All rights reserved.
PII: S0022-3115(02)01307-7

this system constantly change during the process. It is possible to point out some other analogous systems:

1. Production of silver halides by the double-jet technique [7–9], where the rate of addition of components is a controlling parameter of the process.
2. Deposition of thin films where the substrate surfaces may be considered as a two-dimensional solution in which the deposited monomers segregate to form grains. Here again the rate of deposition is controlling the final grain size in the films [5].

Based on experimental observations of silver-halides and also on the material-independent computer simulation by Ludwig and Schmelzer [10] a general scheme may be presented for the process of nucleation and growth with constant addition of monomers.

During an initial 'accumulation' period, solute concentration increases linearly with time. At this stage almost no *nucleation* is observed. Then at a certain concentration nucleation becomes significant. Afterwards nucleation stops when the growth of nucleated precipitates reduces the solute concentration slightly. The nucleation stage starts abruptly and also ends abruptly because of the strong dependence of nucleation rate on supersaturation. After the nucleation ends the nucleated precipitates grow by drawing more solute from the solvent matrix. At this stage of 'independent growth' the supersaturation falls. When the supersaturation reaches a sufficiently low value some of the precipitates become unstable and dissolve while others continue to grow. This is the stage of *Ostwald-ripening*. Further, the dissolution of existing precipitates stops completely or at least significantly slows down. The surviving precipitates now continue to grow mainly by consuming the incoming flux of monomers that are added constantly to the system. This late stage may be called 'second independent growth' (SIG).

SIG stage does not appear in the normal first-order phase transitions in the constant composition systems. It is a unique case specific for precipitation with constant addition of monomers. In this study we concentrate on the late stages of precipitation. We are interested in these stages of the process because real reactor experiments usually take long time – months or years, much longer than the time of nucleation in dilute Al–Si alloys [11].

Several authors considered the late stages of precipitation in changing-composition systems. Kharitonova et al. [7] and Leubner [8] used only mass-balance equations without considering the possibility of change of precipitate number. Chakraverty [5] applied the theory of Ostwald-ripening of Lifshitz and Slyozov [12] and Wagner [13] to the changing-composition systems, namely to thin film deposition. Below, we follow Chakraverty [5] to obtain final formulae for the precipitation of radiogenic Si.

2.2. Model for late stages growth

We begin from the general formula for the growth rate of precipitates in moderately supersaturated solutions. The precipitate size distribution is required to obey continuity and mass balance equations. Using dimensional analysis and again mass balance, we obtain the dependence of precipitate size and number on the monomer addition rate and kinetic parameters.

The growth rate of precipitates in a moderately supersaturated solution with small volume fraction of precipitates is given by [6,14]

$$V = \frac{\mathrm{d}R}{\mathrm{d}\tau} = \frac{1}{R^m}\left(\frac{1}{R_\mathrm{c}} - \frac{1}{R}\right),$$

$$\tau \equiv \left[\frac{2\sigma D c_\mathrm{e} \cdot a_\mathrm{m}^{(m-1)}}{c_\mathrm{p}^2 k_\mathrm{B} T}\right] \cdot t, \tag{1}$$

where R is the precipitate radius, σ is the interfacial free energy of the precipitate boundary, c_p is the concentration of the segregating monomers inside the precipitate, T is the temperature and k_B is Boltzman constant. Different values of index m correspond to different mechanisms of growth (for instance, $m = 0$ stands for interface control and $m = 1$ corresponds the case of diffusion controlled growth). a_m is the mechanism-dependent constant with dimensions of length. D is the diffusion coefficient of the segregating monomers. Its value also depends on the growth mechanism. c_e is the equilibrium concentration of solute in the solvent. R_c is the critical radius for which the actual concentration equals the equilibrium concentration at the precipitate boundary. The size distribution of precipitates, f, obeys the continuity equation:

$$\frac{\partial f}{\partial \tau} + \frac{\partial}{\partial R}(V \cdot f) = 0. \tag{2}$$

Since the concentration of solute in the solvent is negligible at the SIG stage of the process, we may write for the time moment t:

$$c_\mathrm{p} \cdot \frac{4\pi}{3} \int_0^\infty f(R) \cdot R^3 \cdot \mathrm{d}R = P \cdot t, \tag{3}$$

where P is the rate of monomer supply or production per unit volume.

Only Eq. (3), is written exclusively for changing-composition systems.

Searching for a long-term self-similar solution [1] of Eq. (2), we use the expressions (see [15]):

---

[1] A self-similar solution is invariant with respect to scaling transformation. See [15].

$$f(R) = \tau^{\alpha} \cdot \Phi(r), \quad R_{\mathrm{c}} = \left(\frac{\tau}{\gamma}\right)^{\beta}, \quad r = \frac{R}{R_{\mathrm{c}}} = R \cdot \left(\frac{\tau}{\gamma}\right)^{-\beta}, \tag{4}$$

where α, β and γ are constants.

For such a solution the distribution of relative precipitate sizes does not change with time, so that the ratio $\overline{R}/R_{\mathrm{c}}$ between the average precipitate size ($\overline{R}$) and the critical size (R_{c}) is time-independent.

Substituting (4) in (1) and (2), the requirement to preserve dimensionality yields $\beta = 1/(m+2)$, as in constant-composition systems [15]. Substituting (4) in (3) yields $\alpha = 1 - 4\beta$. Thus we obtain:

$$\overline{R} \sim R_{\mathrm{c}} \sim t^{1/(m+2)}, \tag{5}$$

$$f(R) = \tau^{(m-2)/(m+2)} \cdot \Psi\left(\frac{R}{R_{\mathrm{c}}}\right). \tag{6}$$

The number of precipitates is given by

$$N = \int_0^{\infty} f(R) \cdot \mathrm{d}R. \tag{7}$$

Substitution of (5) and (6) in (7) yields $N \sim t^{(\alpha+\beta)}$, and we obtain for the growth controlled by the interface:

$$\overline{R} \sim R_{\mathrm{c}} \sim t^{1/2}, \quad N \sim t^{-1/2} \sim \frac{1}{\overline{R}} \tag{8}$$

and for the growth controlled by diffusion:

$$\overline{R} \sim R_{\mathrm{c}} \sim t^{1/3}, \quad N = \text{constant}. \tag{9}$$

Thus it is shown that while the dissolution of smaller precipitates continues in the case of interface-controlled mechanism, in diffusion controlled process the dissolution stops and the number of precipitates stabilizes. Thus in the case of diffusion control mechanism we obtain SIG. Computer simulations of Ludwig and Schmelzer [10] support in principle this conclusion.

Now the constant γ and the scaled distribution function ψ are determined. Substitution of (5) in (1) yields an equation for the relative growth rate:

$$\frac{\mathrm{d}(r^{m+2})}{\mathrm{d}\ln\tau} = (m+2) \cdot \gamma \cdot (r-1) - r^{m+2}. \tag{10}$$

For constant-composition systems the stable solution of Eq. (10) is given in [15] with

$$\gamma = \gamma_0 = \left(\frac{m+2}{m+1}\right)^{m+1}.$$

In this case $r_0 = \gamma_0^{1/(m+1)}$ (see Refs. [12–15]).

For changing-composition systems the analysis of Eq. (10) (as in Ref. [5]) yields the following results: for interface controlled growth $\gamma = \gamma_0 = 2$ as in constant-composition systems [13]. The distribution function resembles the result for constant-composition systems with a perturbation that makes it narrower [5]. Therefore $(\overline{R}/R_{\mathrm{c}}) \approx (8/9)$ as in constant-composition systems [13]. Thus:

$$\overline{R} = \frac{8}{9}\left(\frac{\tau}{2}\right)^{1/2}. \tag{11}$$

For diffusion controlled growth $\gamma > \gamma_0 = 4/9$ and after long enough time all precipitates achieve a uniform relative size, $r_1 > r_0 = 3/2$. r_1 is the largest real and positive root of Eq. (10) and may be presented as a function of γ. The resulting expression for the precipitate radius [2] is:

$$R = \left(\frac{3\tau}{2}\right)^{1/3} \cdot g\left(\frac{\gamma}{\gamma_0}\right), \tag{12}$$

where g is a function defined by

$$g(x) \equiv (x)^{1/6} \cdot 2\cos\left[\frac{\pi}{3} - \frac{1}{3}\arctan(x-1)\right].$$

The above results are similar to the analysis of thin film systems [5].

The number of precipitates may be now calculated by applying the mass balance equation (3). Replacing the size distribution in (3) by a delta function, centered in $\overline{R}$, substituting (11) and (12) to (3) and returning to the unscaled time variable t we obtain for processes controlled by the interface:

$$N \approx \frac{1}{\pi} \cdot c_{\mathrm{p}}^2 \cdot \left(\frac{k_{\mathrm{B}}T \cdot a_1}{\sigma c_{\mathrm{e}} \cdot D}\right)^{3/2} \cdot \frac{P}{t^{1/2}} \approx \frac{1}{\pi} \cdot \frac{c_{\mathrm{p}} k_{\mathrm{B}} T \cdot a_1 \cdot P}{\sigma c_{\mathrm{e}} \cdot D} \cdot \frac{1}{\overline{R}} \tag{13}$$

and for diffusion-controlled processes:

$$N = \frac{1}{4\pi} \cdot \frac{c_{\mathrm{p}} k_{\mathrm{B}} T \cdot P}{\sigma c_{\mathrm{e}} \cdot D} \cdot \left[g\left(\frac{\gamma}{\gamma_0}\right)\right]^{-3}. \tag{14}$$

The result for diffusion-controlled process still contains the undetermined parameter γ (similar to Leubner's work [8], where the corresponding undetermined parameter is $\overline{R}/R_{\mathrm{c}}$). In principle γ may depend on P, D and thermodynamic parameters. Nevertheless, experimental results with silver-halides [7–9] and the simulations of Ludwig and Schmelzer [10] show that $N \sim (c_{\mathrm{p}} k_{\mathrm{B}} T \cdot P)/(\sigma c_{\mathrm{e}} \cdot D)$. This means that the dependence of $g(\gamma/\gamma_0)$ on the various

---

[2] Note that even if is very close to γ_0 (but slightly larger), the relation $\overline{R} = R_{\mathrm{c}} = (4\tau/9)^{1/3}$ which holds for constant-composition systems, is not recovered from formula (12). It is so because the uniform precipitate size in (12) corresponds to the maximum precipitate size in the distribution, not to the average size.

parameters must be rather weak. If so, we may anticipate that at least the order of magnitude of N will be given by

$$N = \frac{1}{4\pi} \cdot \frac{c_p k_B T \cdot P}{\sigma c_e \cdot D}. \tag{15}$$

Our result for interface-controlled process is different from the corresponding result of Leubner [8] because we have taken into account the variation in precipitate number in the mass balance equation.

2.3. Application to precipitation of radiogenic Si

For radiogenic Si the production rate P may be evaluated by integrating the cross-section for Si production over the whole neutron spectrum. In practice P is proportional to the thermal flux, and the amount of Si produced is proportional to the $\Phi_{th} \cdot t$, which is the thermal neutron fluence. If precipitates are assumed uniform in size (as predicted by the diffusion-control model) and if we neglect the Si atoms in the matrix or in other precipitate phases, we may write a correlation between the precipitate size, the thermal fluence and the precipitate number N:

$$N = 4.2 \times 10^{-29} \cdot \frac{(\Phi_{th} \cdot t)}{d^3}, \tag{16}$$

where d is the precipitate diameter, Φ_{th} is the flux of thermal neutrons and t is the irradiation time. The numerical prefactor (for Si) was calculated using results obtained at reactor ORR, which imply 0.2 wt% Si produced by thermal neutron fluence of 10^{26} m^{-2} [3].

Evaluation of the diffusion coefficient of Si in Al under reactor irradiation requires some more assumptions. It is known that diffusion at low temperatures is stimulated by irradiation [16] because the diffusion coefficient for substitutional diffusion is proportional to vacancy concentration. We proceed from the fact that in the considered case the actual vacancy concentration is much larger than the thermal equilibrium value. Also, the irradiation temperatures (Table 1) are homologous temperatures of 0.33–0.36 T_m at which the vacancies are mobile even without irradiation. At the relatively low temperatures and in materials with a large concentration of non-radiation and radiation-induced complex defects the sink-dominated vacancy annihilation seems more probable in comparison with the vacancy-interstitial recombination. We suggest that just such situation is realized in the considered case.

When the dominant mechanism for vacancy annihilation is their migration to sinks, vacancy concentration is proportional to fast neutron flux, whereas when the vacancies annihilate primarily by recombination with interstitials, the vacancy concentration is proportional to the square root of the fast flux [16]. Thus, for sink-dominated vacancy annihilation Eq. (15) leads to:

$$N \sim \frac{P}{D} \sim \frac{\%\text{Si}}{DPA} \sim \frac{\Phi_{th}}{\Phi_f}, \tag{17}$$

where Φ_f is the flux of fast neutrons, %Si is the percentage of Si produced and DPA is the number of displacements per atom.

For recombination-dominated vacancy annihilation, the analogous result is

$$N \sim \frac{P}{D} \sim \frac{\%\text{Si}}{\sqrt{DPA}} \sim \frac{\Phi_{th}}{\sqrt{\Phi_f}}, \tag{18}$$

Eqs. (17) and (18) manifest the spectral effect found by Farrell [4].

Above we use an implicit assumption that it is possible to neglect the precipitate dissolution caused by the fast neutron bombardment. It seems reasonable to expect that the locally dissolved Si atoms will return soon enough to their parent precipitates, so that this mechanism will not affect substantially the overall supersaturation of Si.

As it will be shown in the Section 3, the mechanism of the interface-controlled growth is inconsistent with experiments for the precipitation of radiogenic Si.

3. Comparison with experiment and discussion

We compared theoretical predictions with experimental results available from the literature. Results obtained by different authors at different nuclear reactors, ORR [3], Mayer and Morris at SAFARI [17], Mitchell at HIFAR [2] where the fluxes were evaluated by Robinson [18], Van Witzenburg and Mastenbroek at HFR [19], Farrell [4] and Packan [20] and Farrel and Richt [21] at HFIR and HFBR [4], are listed in Table 1.

It follows from Table 1 that known experiments do not give the complete data concerning all parameters of irradiation. The nature of the spectrum of different reactors is specified only by a ratio of thermal and fast neutron fluxes, where thermal neutrons are usually defined as having energies $E < 0.025$ eV and fast neutrons are defined as having energies $E > 0.1$ MeV. There are no exact records regarding the irradiation temperature, however, most research reactors mentioned in Table 1 operate at temperatures around 50 °C. More data is available on the sizes of precipitates than data regarding precipitate number. In all experiments precipitates on grain boundaries are larger in size than precipitates in the interior region of the grains. At very high fluence irradiation Si segregates not only in fine precipitates but also in other places such as Si-coatings of irradiation produced voids [22]. These phenomena are not accounted in Table 1, and we compiled only in-grain precipitates. Besides the directly measured values the number of precipitates was also calculated using (16).

Table 1
Summary of the experimental results on Si-precipitation in neutron-irradiated aluminium

Reactor and reference	Irradiation temperature (°C)	Flux ratio (Thermal/Fast)	Thermal neutrons flux (Φ_{th}) (10^{18} $n\,m^{-2}\,s^{-1}$)	Fluence ($\Phi_{th} \cdot t$) (10^{26} $n\,m^{-2}$)	Initial impurities or Alloy designation	Precipitate parameters		
						Diameter (d) (nm)	Number (N) (10^{21} m^{-3})	
							Estimated from d and $\Phi_{th} \cdot t$ (16)	Measured
ORR [3]	40–50	1.1	1.1	1.32	Al-1100	10	5.5	5.5
			~5	3.2		14	4.9	5.5
SAFARI [17]	50	2.5	~2	0.0625	Al-0.01%Si	7.5	1.3	0.4
					Al-0.03%Si	6.5	2.7	2
					Al-0.08%Si	6.5	0.6	2.5
					Al-0.4%Si	7	0.9	5
				0.225	Al-0.08%Si	7	0.9	3
					Al-0.4%Si	9	0.8	5
HFR [19]	45–55	0.9	0.6	2	Al-99.9995%	20–30	1.3	–
HIFAR [2,18]	50	10	0.1–1[a]	2.6	Al-1080	5	87	–
HFIR [20]	50–60	1.7–2.5	17	1.7	Al-99.9999%	10	6	–
HFIR [21]	55–65	1.7–2.5	17	23	Al-1100	25	4.2	1.6
HFIR [4]	44–67	1.7–2.5	27	30	Al-6061	~50	1	–
HFBR [4]	55–65	20	6.4	40	Al-6061	~10	167	–

Irradiation times may be estimated by dividing the thermal fluence to the thermal flux.

[a] Estimated according to Ref. [18].

These calculated values refer to the number of precipitates that would have been measured if all the produced Si is in the fine in-grain precipitates.

Data on interdependence of precipitate size and their number are available from experiments of Farrell and King [3] and of Mayer and Morris [17]. With increase of fluence there is an increase in precipitate size while the number of precipitates does not change. This is in contradiction with Eq. (13) and fits the prediction of Eq. (15). Thus, it is reasonable to exclude the interface-controlled mechanism and proceed to check the diffusion-controlled growth mechanism.

We perform a direct comparison of (15) with the representative experimental data obtained at ORR reactor. The input quantities are: $P \cong 0.2 \times 10^{-8}$ wt% $Si\,s^{-1}$, $c_e \cong 10^{-3}$ wt% Si [23], $\sigma \cong 0.2\ J\,m^{-2}$ [24], $k_B T \cong 5 \times 10^{-21}$ J and $N \cong 5 \times 10^{21}\ m^{-3}$. Substituting these quantities in (15), we calculate the diffusion coefficient of Si in neutron irradiated Al: $D \cong 10^{-18}\ m^2\,s^{-1}$. This value is much larger than the ordinary thermally activated diffusion coefficient at low temperatures $D_{th} \cong 10^{-24}$ $m^2\,s^{-1}$ [23]. This is an expected result as follows from the discussion in Section 2.3.

Overall comparison of the theoretical prediction presented by Eq. (17) with experimental results from Table 1 is displayed in Fig. 1.

We always used calculated numbers of precipitates (according to (16)) so that the experimental values being used are really the precipitate sizes and thermal neutron fluences. A straight line, forced to pass through the origin, was fitted to the experimental points. It is seen from Fig. 1 that although the statistics are not large, there is a fair agreement between theory and experiment with $R^2 = 0.92$. For small numbers of precipitates the results exhibit a visible spread. This may be due to masking of the spectral effect [4] by other mechanisms, when the differences in Φ_{th}/Φ_f are small. Temperature variations may be also significant. Differences in the starting composition and the thermomechanical treatment of the aluminum alloys are also important. It may influence the vacancy concentration through the differences in the amount of sinks for vacancies [25,26]. Besides, experimental errors in measurement of small sizes and numbers of precipitates are naturally larger. Nevertheless, despite the many differences between various experiments, the precipitates number is still correlated with Φ_{th}/Φ_f, as seen in Fig. 1.

Note that small precipitates (and thus the large number of precipitates) were detected at reactors HIFAR and HFBR where the irradiation took long times. Nevertheless, the intuitive expectation is that due to Ostwald-ripening low-flux long-time irradiation would produce larger precipitates for the same fluence. The present model copes with this difficulty because it predicts that after the precipitation process enters the SIG stage the irradiation times do not affect the precipitate number.

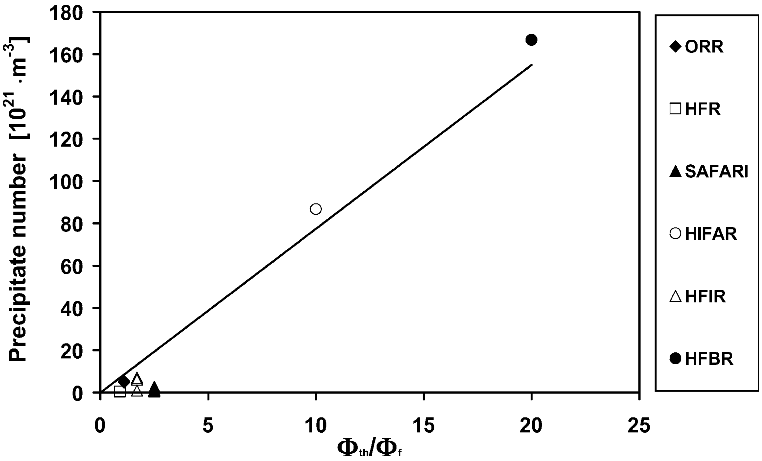

Fig. 1. Comparison between theory and experiment. The line is fitted by least-squares method and is forced to pass through the origin of the axes, $R^2 = 0.92$. The ordinate is the number of precipitates per unit volume. The abscissa is the ratio of fluxes of thermal and fast neutrons.

It follows from Eq. (17) that the number of precipitates is determined only by flux ratio Φ_{th}/Φ_f and not by absolute value of the fluxes and irradiation time.

Eqs. (17) and (18) are valid only for experiments that are conducted at the same temperatures. Determination of the temperature dependence of radiation-stimulated diffusion requires more detailed knowledge of the diffusion mechanism. Study of this problem is in progress.

4. Conclusion

1. We performed an investigation of late stages of precipitation processes with constant rate of addition of monomers. It is shown that different physical processes, such as precipitation of Si in Al under reactor irradiation, deposition of thin films on various substrates and formation of silver halides, have the same kinetics and identical mathematical description.
2. Two limiting cases are studied: (a) the growth of precipitates is controlled by the diffusion or (b) by the reaction at the precipitate surface. We have taken into account the variation of number of particles in the balance equation, and thus obtained more precise results as compared with [8].
3. We found that in reactor conditions, which are characterized by small rate of the addition of monomers and by long experimental time, the growth of precipitates is limited by diffusion of Si in Al the matrix. In these conditions Ostwald-ripening stops and the precipitates grow independently (SIG).
4. We estimate that the diffusion coefficient of Si in Al under reactor irradiation is much larger than the thermal diffusion coefficient at the same low temperatures, This effect is explained by the excess vacancy concentration under irradiation and their radiation-accelerated diffusion. The assumption that diffusion coefficient is proportional to the fast neutron flux (and accordingly that the vacancy annihilation is sink dominated) is proven successfully by comparison of our results with experimental data.
5. The model reasonably fits experimental results obtained at various reactors and allows to quantitative evaluation of the spectral effect on Si precipitation in neutron-irradiated aluminum [4].

Acknowledgements

We are grateful to Dr A. Munitz of NRCN for introducing us to the subject, for numerous stimulating discussions and useful recommendations. We also wish to thank Professor D. Fuks and Mr G. Frank for useful comments.

References

[1] K. Farrell, J.O. Stiegler, R.E. Gelbach, Metallography 3 (1970) 275.
[2] D.R.G. Mitchell, Nucl. Instrum. and Meth. B 140 (1998) 107.
[3] K. Farrell, R.T. King, Metall. Trans. 4 (1973) 1223.
[4] K. Farrell, Mater. Res. Soc. Symp. Proc. 373 (1995) 165, Materials Research Society.
[5] B.K. Chakraverty, J. Phys. Chem. Solids 28 (1967) 2401; B.K. Chakraverty, J. Phys. Chem. Solids 28 (1967) 2413.
[6] V.V. Slezov, J.W.P. Schmelzer, in: J.W.P. Schmelzer, G. Röpke, V.B. Priezzhev (Eds.), Nucleation Theory and Applications, JINR, Dubna, 1999, p. 6; V.V. Slezov, J. Schmelzer, Ya.Y. Tkach, J. Chem. Phys. 105 (1996) 8340.

[7] A.I. Kharitonova, B.I. Shapiro, K.S. Bogonolov, Zh. Nauchn. Prikl. Fotogr. Kinematogr. 24 (1979) 34.

[8] I.H. Leubner, J. Phys. Chem. 91 (1987) 6069;
J. Img. Sci. Technol. 37 (1993) 268;
Curr. Opinion Coll. Interface Sci. 5 (2000) 151.

[9] T. Sugimoto, J. Coll. Interface Sci. 150 (1992) 208.

[10] F.-P. Ludwig, J. Schmelzer, Z. Phys. Chem. 192 (1995) 155.

[11] E. Ozawa, H. Kimura, Acta. Metall. 18 (1970) 995.

[12] I.M. Lifshitz, V.V. Slyozov, Sov. Phys. JETP 8 (1959) 331;
J. Phys. Chem. Solids 19 (1961) 35;
E.M. Lifshitz, L.P. Pitaevskii, Physical Kinetics, Pergamon Press, Oxford, 1981 (Chapter 12).

[13] V.C. Wagner, Z. Electrochem. 65 (1961) 581.

[14] V.V. Slyozov, V.V. Sagalovich, Sov. Phys. Usp. 30 (1987) 23.

[15] Meerson, Phys. Rev. E 60 (1999) 3072.

[16] B.T. Kelly, Irradiation Damage to Solids, Pergamon Press, Glasgow, 1966.

[17] R.M. Mayer, E.T. Morris, J. Nucl. Mater. 71 (1977) 36.

[18] G.S. Robinson, Australian Nuclear Science and Technology internal report, LH87/1067, 1988.

[19] W. Van Witzenburg, A. Mastenbroek, J. Nucl. Mater. 133&134 (1985) 553.

[20] N.H. Packan, J. Nucl. Mater. 40 (1971) 1.

[21] K. Farrell, A.E. Richt, in: J.A. Sprague, D. Kramer (Eds.), Effects of Radiation on Structural Materials ASTM STP 683, American Society for Testing Materials, 1979, p. 427.

[22] K. Farrell, J. Bentley, D.N. Braski, Scr. Metall. 11 (1977) 243.

[23] K. Farrell, J.T. Houston, J. Nucl. Mater. 83 (1979) 57.

[24] C.-H. Tung, C.-T. Chang, H.-C. Chang, S. Chiu, B. Kok, L.-H. Chang, J. Appl. Phys. 68 (1990) 1592.

[25] K. Farrell, in: Dimensional Stability and Mechanical Behaviour of Irradiated Metals Metals and Alloys, Proceedings of Brighton Conference, 11–14 April 1983, British Nuclear Energy Society, London, p. 73.

[26] L.K. Mansur, Nucl. Tech. 40 (1978) 5.